

Gating of the polycystin ion channel signaling complex in neurons and kidney cells

Patrick Delmas,* Surya M. Nauli,[†] Xiaogang Li,[†] Bertrand Coste,* Nancy Osorio,* Marcel Crest,* David A. Brown,[‡] and Jing Zhou[†]

*Intégration des Informations Sensorielles, CNRS, UMR 6150, Faculté de Médecine, IFR Jean Roche, Bd. P. Dramard, 13916 Marseille cedex 20, France; [†]Renal Division, Department of Medicine, Brigham and Women's Hospital and Harvard Medical School, Boston, Massachusetts 02115, USA; [‡]Wellcome Laboratory for Molecular Pharmacology, Department of Pharmacology, University College London, Gower Street, London WC1E 6BT, UK

Corresponding author: Patrick Delmas, Intégration des Informations Sensorielles (UMR 6150), Faculté de Médecine, IFR Jean Roche, Bd. P. Dramard, 13916 Marseille Cedex 20. E-mail: delmas.p@jean-roche.univ-mrs.fr

Corresponding author for materials: Jing Zhou, Harvard Institutes of Medicine, Room 522, 4 Blackfan Circle, Boston, MA 02115, USA. E-mail: zhou@rics.bwh.harvard.edu

ABSTRACT

Mutations in either polycystin-2 (PC2) or polycystin-1 (PC1) proteins cause severe, potentially lethal, kidney disorders and multiple extrarenal (including brain) disease phenotypes. PC2, a member of the transient receptor potential channel superfamily, and PC1, an orphan membrane receptor of largely unknown function, are thought to be part of a common signaling pathway. Here, we show that in rat sympathetic neurons and kidney cells, coassembly of full-length PC1 with PC2 forms a plasmalemmal ion channel signaling complex in which PC1 stimulation simultaneously activates PC2 ion channels and G_{i/o}-proteins. PC2 activation occurs through a structural rearrangement of PC1, independent of G-protein activation. Thus, PC1 acts as a prototypical membrane receptor that concordantly regulates PC2 channels and G-proteins, a bimodal mechanism that may account for the multifunctional roles of polycystin proteins in fundamental cellular processes of various cell types.

Key words: polycystic kidney disease • polycystin-1 • polycystin-2 • G-protein • Ca²⁺-permeable channel

Polycystins form an expanding family of proteins that are widely expressed in various cell types but whose cellular functions remain poorly defined (1). Mutations in the human genes *PKD1* and *PKD2* that encode polycystin-1 (PC1) and polycystin-2 (PC2), respectively, lead to autosomal dominant polycystic kidney disease (ADPKD), an inherited disorder that is the most common cause of renal failure in people. ADPKD is characterized by the progressive development of fluid-filled cysts in the kidney, accompanied by several extrarenal manifestations, including hepatic and brain cysts, cardiac valvular abnormalities, and cerebral and aortic aneurysms (2, 3). Mutations in *PKD1* account for the vast majority of patients with ADPKD, whereas mutations in *PKD2* constitute a less prevalent genetic cause of ADPKD (4).

PC1 is an integral membrane glycoprotein of ~4300–4500 amino acids that is composed of 11 transmembrane domains, a large N-terminal extracellular region containing several adhesive domains, and an intracellular C-terminal region of ~225 amino acids (5, 6). When expressed alone, it appears to act as an atypical, orphan membrane receptor from its ability to activate G-proteins (7, 8) and c-Jun N-terminal kinase (9) via its C-terminal end. PC2 is a smaller (1000 amino acids) protein with sequence homology to the α -subunit of neuronal voltage-gated Ca^{2+} channels and to transient receptor potential channels (TrpC) (10) and forms a Ca^{2+} -permeable, nonselective cation channel of large conductance when functionally reconstituted in lipid bilayer or in oocyte expression systems (11–13).

It is likely that, in vivo, PC1 and PC2 coassemble to form a heteromeric polycystin complex (14). This is supported by the fact that mutations in either *PKD1* or *PKD2* genes produce virtually identical clinical symptoms (4). However, the precise modus operandi of the complex is unclear. Several limitations have rendered studies of polycystin functions difficult, including the low levels of expression of endogenous PC1 in native cells and the low success rate of experiments directed at expression of recombinant full-length polycystins (15). To overcome these limitations, we have overexpressed polycystin proteins in sympathetic neurons (7). These neurons provide a variety of well-characterized endogenous ion channels that can be used as cell-signaling readouts (16–18) and readily express the large (~14 kb) polycystin transcripts (7).

Here, we demonstrate that PC1 and PC2 form functionally associated “subunits” of a heteromultimeric signaling complex that functions either as a Ca^{2+} -permeable cation channel or as a G-protein-coupled receptor. Within these complexes, PC1 acts as a cell surface receptor that controls the gating of the PC2 channel via a structural rearrangement, independently of G-protein activation, whereas association with PC2 regulates the G-protein-coupling activity of PC1. This constitutes a novel form of heteromeric receptor function.

MATERIALS AND METHODS

DNA constructs

hPKD1, mPKD1, mPKD1_{C193}, mPKD2, and mPC2R742X cDNAs were subcloned into pcDNA3.1 expression vectors and were described previously (7, 19). hPKD1 construct contains a partial 8428 bp cDNA of human PKD1, encoding the C-terminal 2492 amino acid of PC1, whereas mPKD1 and mPKD2 constructs encode the entire mouse polycystin-1 (4303 amino acids) and the entire mouse PC2, respectively. mPC1_{C193} was generated by a deletion of the last 193 amino acids of mouse polycystin-1. mPC2 R742X mutant lacks the C-terminal 226 amino acid of PC2, which includes the EF-hand and the PC1 interaction domain.

Cultures of neurons and cDNA delivery

Sympathetic neurons were isolated from Sprague Dawley rat superior cervical ganglions (SCGs) and cultured on glass coverslips as previously described (20). DNA plasmids were diluted to 100 $\mu\text{g}/\text{ml}$ in Ca^{2+} -free solutions (pH 7.3) containing 0.2% FITC-dextran (70 kDa) and were pressure-injected into the nucleus of SCG neurons as previously described (21, 22). Cells were maintained in culture for a further 2 days before recording.

Culture of kidney cells

Kidneys of E15.5 embryos were dissociated, incubated with collagenase (1 mg/ml), and then plated in Dulbecco's modified Eagle's medium containing 2% fetal bovine serum, 0.75 $\mu\text{g/l}$ interferon- γ , 1 g/l insulin, 0.67 mg/l sodium selenite, 0.55 g/l transferrin, 0.2 g/l ethanolamine, 36 ng/ml hydrocortisone, 0.10 μM 2,3,5-triiodo-L-thyronine, 100 units penicillin-G (base) in combination with 0.3 mg/ml additional glutamine, 100 μg of streptomycin sulfate, and 0.1 mM citrate. For Ca^{2+} microfluorometry, cells were grown for at least 2 days in the absence of interferon- γ to induce optimal differentiation. As described previously (23), *Pkd1*^{del34} is created by replacing exon 34 of *Pkd1* by a neomycin-resistant gene. This mutation is predicted to result in a truncated PC1 protein of 3532 residues, lacking the C-terminal half of the transmembrane domains and the entire C-terminal intracellular domain. Tubular epithelial cells were isolated from the kidneys of this mouse model carrying the large T antigen. Cells containing distal tubule marker (dolichos biflorus agglutinin, DBA) were then purified (24) and maintained at 33°C in the proliferative media described above. Once the cells reached ~90% confluence, they were differentiated at 37°C in the media with 5% serum for 3 days.

Cytosolic microinjection of anti-mPC2 antibody

Micropipets with resistance of 70 M Ω were filled with filtered intracellular solution containing the anti-mPC2 antibody at 1/100 plus 0.2% TRITC-dextran (10 kDa) (21).

Whole-cell recording

Neurons were recorded using the perforated patch (PC2 current) or patch-ruptured (Ca^{2+} currents) whole-cell variants of the patch-clamp technique. For recording PC2 channel current, the external solution consisted of (in mM) NaCl, 110; NaHCO₃, 23; KCl, 3; MgCl₂, 1.2; CaCl₂, 0.1–0.5; HEPES, 5; glucose, 11; and tetrodotoxin (TTX), 0.0005 (bubbled with a 95% O₂/5% CO₂ mixture, pH 7.4), and the intracellular solution was amphotericin-B (0.1 mg/ml in DMSO); K⁺ acetate, 90 mM; KCl, 30 mM; MgCl₂, 3 mM; and HEPES, 40 mM (adjusted to pH 7.3 with KOH, 290 mOsmol/l). For Ca^{2+} currents, the internal solution was (in mM) NMDG, 109; CsCl, 14; HEPES, 10; EGTA, 11; CaCl₂, 0.5–1; phosphocreatine, 0.1; MgATP, 4; and Na₃GTP, 0.2 (pH 7.3), and the external solution was as above plus 2 mM CaCl₂. Pipets were coated with Sylgard and had resistance of 2–3.5 M Ω . Currents were measured with an Axopatch 200A amplifier, filtered at 1–5 kHz and leak subtracted. Cell membrane capacitance and series resistance compensations were applied. Experiments were performed at 30–32°C, and drugs were applied by using a gravity-fed perfusion system (10 ml/min). *N*-ethylmaleimide was applied at 20 μM for at least 2 min, and PTX (*Bordetella pertussis* toxin) was incubated for 24 h at 1 $\mu\text{g ml}^{-1}$. Data were expressed as the mean \pm SE. ANOVA and Student's *t* test were applied to determine the statistical significance. Differences were considered significant if $P < 0.05$.

Cell-attached patch recording

Sylgard-coated pipets had resistances of 12–20 M Ω when filled with (in mM) NaCl, 135; HEPES, 10; TEA-Cl, 11; 4-aminopyridine, 3; and TTX, 0.0005 (pH 7.3 with TEAOH). Voltages are given in the normal convention and were not corrected for junction potentials. Open probability (p_o) was calculated from 1 min period recording in patches containing only one channel. Single channel current levels were measured by all-points histograms, and the slope

conductance was calculated from linear regression. The drugs La^{3+} and amiloride were dissolved in the pipet solution before recording.

Measurement of intracellular calcium

Coverslips with mouse kidney epithelial cells were loaded for 30 min with 5 μM Fura-2AM at room temperature in buffer containing (in mM) 132 NaCl, 4.2 NaHCO_3 , 5.9 KCl, 1.4 MgSO_4 , 1.2 Na_2HPO_4 , 1.6 CaCl_2 , 11 dextrose, and 10 HEPES (pH 7.4). The coverslips were then placed in a thermostatted quartz cuvette, and MR3 antibody was used at a final dilution of 1:50. Excitation monochrometers were centered at 340 and 380 nm, and emission light was collected at 510 nm through a wide-band emission filter. The 340/380 excitation ratio of emitted light was used to calculate relative cytosolic Ca^{2+} .

Immunoblotting

Full-length myc-tagged mPC2 was transiently transfected into HEK293 cells. Precleared cell lysates were incubated with the anti-myc antibody at 4°C for 12 h and immunocomplexes were captured with protein-A beads for 2 h. The beads were washed, and bound proteins were then fractionated by SDS-PAGE followed by Western blot analysis. Western blots were probed with the anti-mPC2 antibody (44-62) before incubation with horseradish peroxidase-coupled antibody. Immobilized antibodies were detected by ECL.

Immunofluorescence

For primary neuronal cultures, cells were fixed with 4% paraformaldehyde for 20–25 min at room temperature, followed by 5 min treatment with Triton X (0.1%). After incubation with bovine serum albumin and phosphate-buffered saline (PBS), neurons were incubated with primary antibodies for 1 h, washed, and then stained with FITC- or TRITC-conjugated secondary antibodies (1/200) for 35 min. Fluorescence images were sequentially acquired to avoid signal crossover and were obtained by confocal laser scanning microscopy. The anti-human PC1 polyclonal antibody MR3 (25) was used at 1:500, the N-terminal anti-mPC2 (44-62) was used at 1/800, and the anti- $\alpha 1\text{B}$ Ca^{2+} channel subunit antibodies (ACC-002, Alamone) was used at 1/200.

For staining of kidney epithelial cells, cells were grown to full confluence, fixed with 3% paraformaldehyde containing 2% sucrose in PBS (pH 7.2), and superficially permeabilized with 1% Triton X for <1 min. After they were washed with PBS, cells were incubated with the anti-PC2 antibody (1:1000 dilution) overnight at 4°C and subsequently with FITC labeled anti-rabbit (1:500 dilution) secondary antibody for 1 h at room temperature (25). Antibody to the membrane marker (ZO-1), a kindly gift from Dr. Bradley Denker (Renal Division, Harvard Medical School, Boston, MA) was applied without any dilution for 1 h at room temperature followed by Texas Red labeled anti-rat antibody (1:500) at room temperature for 1 h. Confocal fluorescence microscopy was used to observe and micrograph the cells. The micrographs were then analyzed for z-section (z-stack) using metaimage analysis software Metamorph v.4.6.7. All cell culture supplements were obtained from Invitrogen (Carlsbad, CA), except for interferon- γ , hydrocortisone, and 2,3,5-Triido-L-thyronine, which were obtained from Sigma (St. Louis, MO).

RESULTS

Reconstitution of the PC1/PC2 complex in sympathetic neurons

To reconstitute polycystin complexes, we intranuclearly microinjected sympathetic neurons with *mPKD2* cDNA alone or in combination with *hPKD1* cDNA or C-terminally truncated *hPKD1* cDNA (*hPC1*_{C193}). Confocal immunostaining performed 48 h after gene delivery showed that mPC2 staining was restricted to the ER in cells microinjected with *PKD2* cDNA alone. In contrast, mPC2 was also found concentrated in the outer membrane when coexpressed with hPC1 ([Fig. 1A](#)), in agreement with previous reports in CHO cells (11). Combined visualization of mPC2 and hPC1 revealed multiple areas of colocalization of the two proteins in the cell surface. Coexpression of the C-terminal truncation mutant *hPC1*_{C193}, which lacks the coiled-coil interaction domain with PC2, failed to bring PC2 to the cell surface, although the PC1 mutant remained targeted to the plasma membrane ([Fig. 1B](#)). Furthermore, mPC2 was coimmunolabeled with the α_{1B} Ca²⁺ channel subunit, a typical plasma membrane protein, when coexpressed with full-length hPC1 ([Fig. 1C](#)). In the absence of PC1, mPC2 was not targeted to the plasma membrane and was retained intracellularly ([Fig. 1D](#)).

Ionic currents produced by the PC1/PC2 complex

Whole-cell perforated patch-clamp recordings were made 48 h after cDNA delivery in the presence of low external Ca²⁺ concentrations (0.1–0.5 mM) in order to prevent Ca²⁺ loading through constitutive channel activity. Cells coexpressing mPC2 and hPC1 displayed a standing inward current with a mean amplitude of -2.15 ± 0.6 pA/pF ($n=11$) at -60 mV that was inhibited by amiloride (see below) and that was absent in uninjected cells, mock cells (expressing the green fluorescent protein), or cells expressing hPC1 alone (-0.11 , -0.14 , and -0.19 pA/pF, respectively; $n=5-8$) ([Fig. 2A-C](#)). Consistent with the lack of plasma membrane localization of mPC2 when expressed alone, only a tiny, if any, amiloride-sensitive inward current was seen in cells expressing mPC2 (-0.19 ± 0.1 pA/pF, $n=9$) ([Fig. 2B](#)).

The hPC1/mPC2 inward current had a reversal potential of -2 ± 3 mV, was voltage-independent between -80 and -20 mV, and was prevented by isosmotically substituting external Na⁺ by sucrose ($n=8$). Relative permeability of Na⁺ to K⁺ to Ca²⁺, calculated using the bionic equation modified from the Goldman-Hodgkin-Katz equation, was 1:0.98:0.57. mPC2 formed the channel pore in the hPC1/mPC2 complex because the current was depressed by amiloride (IC_{50} 42 ± 8 μ M, $n=8$) and La³⁺ (IC_{50} 62 ± 9 μ M, $n=6$), two known blocking agents of PC2 channels (11, 12) ([Fig. 2](#)), and was also suppressed by cytoplasmic microinjection of an antibody raised against an intracellular epitope (amino acids 44–62) located on the N terminus of mPC2 ($n=5$ out of 5) (data not shown, but see [Fig. 4D](#)).

Expression of the mPC2 mutant R742X lacking the C-terminal 226 amino acids, which includes the PC1 interaction domain and the ER retention signal, produced a significantly larger amiloride-sensitive inward current (-5.4 ± 0.5 pA/pF) than that obtained in hPC1/mPC2-expressing cells ([Fig. 2D, 2E](#)). The mPC2 R742X current had a similar reversal potential (-1 ± 2 mV) and pharmacology (amiloride IC_{50} 36 ± 7 μ M, $n=5$; La³⁺ IC_{50} 57 ± 5 μ M, $n=5$) to the current generated by PC1/PC2 complexes.

Microscopic properties of the PC1/PC2 ion channel complex

The larger current generated by PC2 R742X vs. PC1/PC2 suggests that binding of PC1 to PC2 might control the gating of the channel, as well as its plasmalemmal expression. To test this, we made single channel recordings from somatic membranes of cells expressing either hPC1/mPC2 or mPC2 R742X channels, using external Na^+ and internal K^+ as charge carriers. These experiments revealed cation channel currents with main chord conductances of 90–130 pS in both cell types (Fig. 3A–D). These channels were most frequently encountered in cells coexpressing hPC1/mPC2 (14 out of 32 patches, Fig. 3A) and less frequently in cells expressing mPC2 R742X (9 out of 41 patches, Fig. 3B). Channel activities were suppressed by amiloride or La^{3+} added to the patch pipet (lower traces in Fig. 3A, B) and were not detected in untransfected cells ($n=41$), mock cells (29 patches), or cells expressing hPC1 alone (34 patches). Note that amiloride acted as a fast blocker of channel activity reducing the conductance but not the open probability (p_o) of the channels, a characteristic trademark of amiloride action on PC2 (12).

The open probability of single mPC2 R742X channels was significantly higher ($P<0.001$, 6 active patches for each) than that of hPC1/mPC2 channels (Fig. 3E; mean p_o at -40 mV 0.37 for mPC2 R742X and 0.11 for hPC1/mPC2). Although not investigated extensively, the low p_o of the hPC1/mPC2 channel complex might be due to both an increase in the closed dwell-time and an alteration of the kinetic behavior. The overall properties of single mPC2 channels observed here are in good agreement with those of PC2 reconstituted in lipid bilayers (12).

Binding of antibodies to extracellular N-terminal domains of PC1 activates PC2 channels

The above data suggest that PC1 interaction with PC2 negatively regulates PC2 channel activity. To study the dynamic regulation of PC2 by PC1, we used the polyclonal anti-hPC1 antibody MR3 as a putative ligand of hPC1. MR3 binds to amino acids 2938–2956 on the N-terminal extracellular domain of hPC1 near the receptor for egg jelly (REJ) domain (25).

Local application of MR3 to cells coexpressing hPC1/mPC2 complexes induced a slowly developing inward current (-8.6 ± 0.8 pA/pF, 15 cells out of 17). This again was carried by mPC2 because it was voltage-independent, had the same reversal potential as the mPC2 current (-3 ± 2 mV), was blocked by amiloride (Fig. 4C), and was suppressed by cytosolic microinjection of the mPC2 antibody (Fig. 4D). MR3 did not induce any currents when applied to mock cells ($n=7$ out of 7) or to cells expressing either hPC1 or mPC2 alone ($n=8$ and 14, respectively) (Fig. 4A, B). Rabbit preimmune serum had no effect on hPC1/mPC2-expressing cells ($n=5$). We confirmed the specificity of the anti-mPC2 antibody used in functional experiments by immunoprecipitating mPC2 subunits overexpressed in HEK293 cells (inset in Fig. 4D). In addition, MR3 had no significant effect on membrane currents of cells coexpressing hPC1_{C193}/mPC2 ($n=4$) or hPC1/mPC2 R742X ($n=6$) (Fig. 4E, F), indicating that integrity of the C-terminal tails of both PC1 and PC2 is required for the functionality of the polycystin complex.

Because our *hPKDI* construct lacks a significant portion of the extensive extracellular regions, we tested whether PC2 activation by PC1 could be replicated using full-length PC1. For this, full-length mPC1 and mPC2 were coexpressed and an antibody that binds to the N-terminal 866–882 amino acids of mPC1 was used as ligand (Fig. 5). Activation of mPC2 current in response to local application of the mPC1 antibody (1/100) was detected in 5 out of 8 cells tested. The mPC1 antibody-induced current (-4.5 ± 0.4 pA/pF) had the same I-V relationship and reversal potential as the MR3-induced current (Fig. 5B, C). Likewise, it was suppressed by amiloride (100 μM ,

$n=4$) and La^{3+} (100 μM , $n=3$; [Fig. 5C](#)) and by preloading the cells with the N-terminal mPC2 antibody ($n=5$) ([Fig. 5B, D](#)).

Parallel activation of PC1/PC2 channel complex and $G_{i/o}$ -type G-proteins by MR3

Because we (7) and others (8) have shown that PC1 can constitutively activate G-proteins, we tested whether enhancement of PC2 activity was accompanied by G-protein activation. For this, we used endogenous N-type Ca^{2+} channels (I_{Ca}) as sensors for activated G-proteins (26, 27). In cells expressing hPC1 alone, Ca^{2+} currents were inhibited through tonic G-protein activation and $G\beta\gamma$ release, as indicated by the strong voltage-dependent current facilitation ([Fig. 6A](#)). Application of MR3 had no significant effect on I_{Ca} in these cells ($n=6$) ([Fig. 6A](#)) or on I_{Ca} recorded in cells expressing mPC2 alone ($n=6$, [Fig. 6B](#)). Coexpression of mPC2 represses this tonic hPC1 modulation of Ca^{2+} currents, so voltage-dependent facilitation was virtually absent in cells coexpressing mPC2 ([Fig. 6A](#), right panel, control traces). MR3 application onto hPC1/mPC2 cells removed this repression and produced a gradual inhibition of Ca^{2+} currents that presented all the characteristic features of $G\beta\gamma$ modulation, that is, slowing in the activation kinetics of I_{Ca} and relief of inhibition by large depolarizing voltages ($n=8$) ([Fig. 6A–C](#)). MR3 no longer inhibited Ca^{2+} currents in the presence of $G\alpha$ -transducin, a potent $G\beta\gamma$ sequestering agent ($n=4$, data not shown) or following 24 h of pretreatment with *pertussis* toxin (PTX) ($n=6$, [Fig. 6D](#)), demonstrating that MR3 activates $G_{i/o}$ -type G-proteins and releases their associated $\beta\gamma$ dimers.

MR3-induced activation of PC2 channel is independent of G-protein signaling

The above data suggest that MR3 causes the rearrangement of the C-terminal domain of PC1, which unmask the PC1 G-protein binding site and leads to G-protein activation. However, G-protein activation was not responsible for MR3-induced PC2 activity, because such activity could still be induced in hPC1/mPC2-expressing cells after pretreatment with PTX ($n=12$, [Fig. 7](#)). Furthermore, bath application of *N*-ethylmaleimide (2 μM , $n=5$), another $G_{i/o}$ -protein uncoupling agent, or intracellular dialysis of GDP- β -S (2 mM, GTP omitted, $n=4$), failed to prevent activation of PC2 currents by MR3 (data not shown). In addition, bath application of U73122 (10 μM for 10 min, $n=7$) and intracellular dialysis of heparin (1 mg/ml, $n=5$) or 8-NH₂-cADPR (50 μM , $n=4$) had no significant effect on the MR3-evoked PC2 current ($0.3 > P > 0.09$). Finally, intracellular injection of the $G\alpha_{q/11}$ antibody CQ1 (1/200) did not affect the responses to MR3 illustrated in [Figure 4](#) ($n=5$). These data suggest that PC1 regulates PC2 channel gating by a mechanism that concomitantly activates G-proteins but that does not require either G-protein or PLC/ Ca^{2+} signaling to occur.

PC1/PC2 complexes in kidney epithelial cells derived from wild-type or *Pkd1* mutant mice

To test whether the mechanism by which PC1 activates PC2 channel is applicable to kidney epithelia, we applied MR3 antibody on kidney epithelia of collecting duct origin (E15.5) and examined Ca^{2+} mobilization. We found that MR3 antibody (1/50), but not normal rabbit serum, evoked a large increase in cytosolic Ca^{2+} concentration in wild-type cells ([Fig. 8A](#)), suggesting that channel activation mechanism in the kidney may be similar to that in our neuronal expression system. Calcium mobilization by MR3 was prevented in Ca^{2+} -free external solution (0 mM Ca^{2+} +1 mM EGTA) and by the application of the blocking antibody p57 (1/50) directed against the external residues 278–428 of mPC2 (24). MR3 response was mediated by PC1 because MR3 failed to generate a Ca^{2+} response in kidney epithelial cells isolated from *Pkd1*^{del34/del34}

homozygous mutant embryos (Fig. 8B). The *del34* mutation is a truncation mutation in *Pkd1*, predicted to truncate PC1 by 836 amino acids, and mimics many mutations found in human ADPKD patients (23, 28). Likewise, MR3 was inactive in kidney epithelial cells isolated from *Pkd1*^{null/null} mutants that lack PC1 (data not shown) (24).

To determine the subcellular expression pattern of PC2 in kidney epithelial cells and its dependence on PC1, we performed immunohistochemistry using the anti-N-terminal PC2 antibody in wild-type and *Pkd1* mutant epithelial cells. PC2 colocalized with the tight junction-associated protein ZO-1 in wild-type cells (Fig. 9). Plasmalemmal localization of PC2 was severely altered in cells isolated from *Pkd1*^{del34/del34} mouse mutants, consistent with the inability for this PC1 mutant to physically bind to PC2. PC2 plasma membrane localization was virtually lost in cells derived from *Pkd1*^{null/null} mutants (Fig. 9).

DISCUSSION

Sympathetic neurons provide a very helpful expression system for studying the functions of recombinant polycystin complexes, because their ion channels can be used as real-time sensors. Using this system, we find that PC1 and PC2 form functionally associated “subunits” of a heteromultimeric receptor-channel signaling complex, in which the association of PC2 represses the endogenous G-protein-activating property of PC1, and conversely PC1 regulates the gating of the PC2 ion channel. This mutual repression can then be relieved by a structural rearrangement induced (in these experiments) by antibody binding to PC1. To our knowledge, this coupling mechanism represents a new type of transduction device that may account for the multifunctional roles of polycystins in the regulation of cell differentiation, proliferation, and ion transport.

The polycystin complex: a multifunctional ion channel/G-protein-signaling complex

Our experiments reconcile previous studies on a naturally occurring PC2 mutation R742X in that PC2 R742X can engage in ion channel activity independently of PC1 (11, 19, 29). Our data also suggest that PC1 is a prerequisite for targeting PC2 to the plasma membrane, although PC2 can also modulate PC1 expression (30). We present direct evidence that PC2 is actually inserted into the plasma membrane and colocalized with PC1. PC1/PC2 complexes then functionally reconstitute a novel surface Ca²⁺-permeant nonselective cation channel, in line with recent data (11). PC2 clearly acts as the ion-translocating component of the complex because the pharmacological and permeation properties of PC1/PC2 ion channel complexes resemble those of recombinant homomeric PC2 or native PC2 from human term syncytiotrophoblasts reconstituted in lipid bilayers (12, 13) and because PC1/PC2 channel activity could be blocked by the anti-mPC2 antibody.

We further show that the two polycystin proteins have reciprocal “stabilizing/inhibitory” effects on each other’s function. We have previously shown that PC2 dampens the ability of PC1 to activate G_{i/o}-proteins (7) (see also Fig. 6) and now provide evidence that PC1 interaction with PC2 inhibits the constitutive activity of the PC2 channel (Fig. 3). Applying an antibody against the N-terminal domains of PC1 may then relieve this inhibition. Thus, the antibody simultaneously enhanced PC2 gating and stimulated PC1-induced G_{i/o}-protein turnover. These effects appear to proceed through a structural rearrangement of the PC1/PC2 complex that requires integral C-termini of both proteins, because C-terminally truncated forms of PC1 and PC2 were unable to reconstitute a functional polycystin complex. Although we cannot exclude the possibility that regulation of PC2 by PC1 was mediated by a yet-unknown second messenger

system, the findings that PC2 modulation is independent of G-protein and PLC signaling, in conjunction with the well-established physical interaction of PC1 and PC2, strongly support the idea that the PC1/PC2 interrelationship occurs via conformational coupling. It is conceivable therefore that the concordant activation of PC2 and G-proteins results from the repositioning of the respective carboxy-terminal tails of PC1 and PC2, leading on one hand to the release of the G-protein binding site of PC1 and, on the other hand, to a conformational change of the PC2 channel. The precise molecular stoichiometry of the polycystin complex is still uncertain. However, given the propensity of PC2 to homodimerize rather than to heterodimerize with PC1 (31, 32), it is plausible that polycystin complex comprises a oligotetrameric PC2 channel bound to a single PC1 protein via C-terminal tethering. Because PC2 has also been identified as an ER protein that can act as a Ca^{2+} -regulated Ca^{2+} channel (33), the intriguing possibility remains that PC1 also plays a role in regulating intracellular PC2.

Our observations further suggest that kidney cells use a comparable molecular mechanism for activation of the PC2 channel. Thus, in kidney epithelia, PC2 was expressed abundantly in the plasma membrane in the presence of integral PC1, and functional coupling of the two could be inferred from the activation of PC2-dependent Ca^{2+} signals in response to PC1 stimulation and by the lack of detectable PC2 activation in *Pkd1^{del34/del34}* and *Pkd1^{null/null}* mutant kidney cells. Collectively, our data suggest that binding of antibodies to the large extracellular domain of PC1 results in conformational change of the polycystin complex that ultimately leads to activation of PC2, a mechanistic molecular sequence that fits well with the recently proposed role of PC1/PC2 complexes as mechano-fluid stress sensors in cilia of embryonic kidney cells (24). Although our mouse embryonic cell lines showed expression of PC2 on both plasma membrane and cilia (24, 34), it remains to be determined whether plasmalemmal PC2 would contribute to signal amplification from ciliary activation. Nonetheless, the present study demonstrates another potential polycystin regulatory pathway, possibly in concert or in parallel with the ciliary pathway.

Paradigmatic nature of the polycystin complex

Overall, our data support the notion that genetic alterations of PC1 or PC2 interfere with the proper assembly, activity, and regulation of the polycystin ion channel signaling complex, and that loss of specific functions of these complexes may provide a possible mechanistic explanation of the pathophysiology of ADPKD. Our proposed mechanism may also be paradigmatic for the function of other polycystin orthologs and related proteins in a variety of tissues. Ca^{2+} -dependent signaling by PC1 is reminiscent of that occurring during the acrosome reaction, a prerequisite for sperm-egg fusion in sea urchin sperm (35). In these cells, it is the receptor REJ3 protein, a membrane glycoprotein sharing domain homology with PC1 that binds to the egg jelly and triggers the acrosome reaction by increasing intracellular Ca^{2+} (36). Of particular relevance is the finding that antibodies raised against external domains of REJ3 produce calcium influx and trigger the acrosome reaction (35), a mechanism that may be phenomenologically related to the one described here for the polycystin complex. Also, the orthologs of PC1 and PC2 in *Caenorhabditis elegans* were found to be expressed in adult male sensory neurons and function in a common mechanosensory pathway during male mating behavior (37, 38). Thus, on the basis of developments reported here, it is conceivable that PC1 and related proteins function as extracellular sensors that regulate Ca^{2+} transport through PC2 or analogous channels. Because polycystins are widely expressed and play multifunctional roles in the regulation of cell differentiation and proliferation as well as ion transport, our data may be of primary relevance for

understanding cyst formation in ADPKD as well as functions of the multiple members of the polycystin gene family in a variety of cells.

ACKNOWLEDGMENTS

This work was supported in part by The Wellcome Trust to P.D. and D.A.B. as well as grants from the National Institutes of Health to J.Z. and from the Centre National de la Recherche Scientifique to P.D. and M.C. We thank Prof. Graeme Milligan (Institute of Biomedical and Life Sciences, University of Glasgow, UK) for the gift of the G $\alpha_{q/11}$ antisera (CQ1) and E. Williams and A. Elia for technical assistance and constructive discussion.

REFERENCES

1. Stayner, C., and Zhou, J. (2001) Polycystin channels and kidney disease. *Trends Pharmacol. Sci.* **22**, 543–546
2. Gabow, P. A. (1990) Autosomal dominant polycystic kidney disease: more than a renal disease. *Am. J. Kid. Dis.* **16**, 403–413
3. Calvet, J. P., and Grantham, J. J. (2001) The genetics and physiology of polycystic kidney disease. *Semin. Nephrol.* **21**, 107–123
4. Wu, G., and Somlo, S. (2000) Molecular genetics and mechanism of autosomal dominant polycystic kidney disease. *Mol. Gen. Metab* **69**, 1–15
5. Hughes, J., Ward, C. J., Peral, B., Aspinwall, R., Clark, K., San Millan, J. L., Gamble, V., and Harris, P. C. (1995) The polycystic kidney disease 1 (*PKD1*) gene encodes a novel protein with multiple cell recognition domains. *Nat. Genet.* **10**, 151–160
6. Sandford, R., Sgotto, B., Aparicio, S., Brenner, S., Vaudin, M., Wilson, R. K., Chisoe, S., Pepin, K., Bateman, A., Chothia, C., et al. (1997) Comparative analysis of the polycystic kidney disease 1 (*PKD1*) gene reveals an integral membrane glycoprotein with multiple evolutionary conserved domains. *Hum. Mol. Genet.* **6**, 1483–1489
7. Delmas, P., Nomura, H., Li, X., Lakkis, M., Luo, Y., Segal, Y., Fernandez-Fernandez, J. M., Harris, P., Frischauf, A. M., Brown, D. A., et al. (2002) Constitutive activation of G-proteins by polycystin-1 is antagonized by polycystin-2. *J. Biol. Chem.* **277**, 11276–11283
8. Parnell, S. C., Magenheimer, B. S., Maser, R. L., Zien, C. A., Frischauf, A.-M., and Calvet, J. P. (2002) Polycystin-1 activation of c-Jun N-terminal kinase and AP-1 is mediated by heterotrimeric G proteins. *J. Biol. Chem.* **277**, 19566–19572
9. Arnould, T., Kim, E., Tsiokas, L., Jochimsen, F., Grüning, W., Chang, J. D., and Walz, G. (1998) The polycystin kidney disease 1 gene product mediates protein kinase C α -dependent and c-jun N-terminal kinase-dependent activation of the transcription factor AP-1. *J. Biol. Chem.* **273**, 6013–6018
10. Mochizuki, T., Wu, G., Hayashi, T., Xenophontos, S. L., Veldhuisen, B., Saris, J. J., Reynolds, D. M., Cai, Y., Gabow, P. A., Pierides, A., et al. (1996) *PKD2*, a gene for

polycystic kidney disease that encodes an integral membrane protein. *Science* **272**, 1339–1342

11. Hanaoka, K., Qian, F., Boletta, A., Bhunia, A. K., Piontek, K., Tsiokas, L., Sukhatme, V. P., Guggino, W. B., and Germino, G. G. (2000) Co-assembly of polycystin-1 and -2 produces unique cation-permeable currents. *Nature* **408**, 990–994
12. González-Perrett, S., Kim, K., Ibarra, C., Damiano, A. E., Zotta, E., Batelli, M., Harris, P. C., Reisin, I. L., Arnaout, M. A., and Cantiello, H. F. (2001) Polycystin-2, the protein mutated in autosomal dominant polycystic kidney disease (ADPKD), is a Ca^{2+} -permeable nonselective cation channel. *Proc. Natl. Acad. Sci. USA* **98**, 1182–1187
13. Vassilev, P. M., Guo, L., Chen, X. Z., Segal, Y., Peng, J. B., Basora, N., Babakhanlou, H., Cruger, G., Kanazirska, M., Ye, C., et al. (2001) Polycystin-2 is a novel cation channel implicated in defective intracellular Ca^{2+} homeostasis in polycystic kidney disease. *Biochem. Biophys. Res. Commun.* **282**, 341–350
14. Newby, L. J., Streets, A. J., Zhao, Y., Harris, P. C., Ward, C. J., and Ong, A. C. (2002) Identification, characterization, and localization of a novel kidney polycystin-1-polycystin-2 complex. *J. Biol. Chem.* **277**, 20763–20773
15. Ong, A. C. M. (2000) Polycystin expression in the kidney and other tissues: complexity, consensus and controversy. *Exp. Nephrol.* **8**, 208–214
16. Ikeda, S. R., Lovinger, D. M., McCool, B. A., and Lewis, D. L. (1995) Heterologous expression of metabotropic glutamate receptors in adult rat sympathetic neurons: subtype-specific coupling to ion channels. *Neuron* **14**, 1029–1038
17. Delmas, P., Wanaverbecq, N., Abogadie, F. C., Mistry, M., and Brown, D. A. (2002) Signaling microdomains define the specificity of receptor-mediated InsP_3 pathways in neurons. *Neuron* **34**, 209–220
18. Delmas, P., and Brown, D. A. (2002) Junctional signaling microdomains: bridging the gap between the neuronal cell surface and Ca^{2+} stores. *Neuron* **36**, 787–790
19. Chen, X.-Z., Segal, Y., Basora, N., Guo, L., Peng, J. B., Babakhanlou, H., Vassilev, P. M., Brown, E. M., Hediger, M. A., and Zhou, J. (2001) Transport function of the naturally occurring pathogenic polycystin-2 mutant, r742x. *Biochem. Biophys. Res. Commun.* **282**, 1251–1256
20. Delmas, P., Brown, D. A., Dayrell, M., Abogadie, F. C., Caulfield, M. P., and Buckley, N. J. (1998) On the role of endogenous G-protein $\beta\gamma$ subunits in Ca^{2+} current inhibition by neurotransmitters in rat sympathetic neurones. *J. Physiol. (Lond.)* **506**, 319–329
21. Delmas, P., Abogadie, F. C., Milligan, G., Buckley, N. J., and Brown, D. A. (1999) $\beta\gamma$ dimers derived from G_o and G_i proteins contribute different components of adrenergic inhibition of Ca^{2+} channels in rat sympathetic neurones. *J. Physiol. (Lond.)* **518**, 23–36

22. Delmas, P., Abogadie, F. C., Buckley, N. J., and Brown, D. A. (2000) Calcium channel gating and modulation by transmitters depend on cellular compartmentalization. *Nat. Neurosci.* **3**, 670–678
23. Lu, W., Peissel B., Babakhanlou, H., Pavlova, A., Geng, L., Fan, X., Larson, C., Brent, G., and Zhou J. (1997) Perinatal lethality with kidney and pancreas defects in mice with a targeted *Pkd1* mutation. *Nat. Genet.* **17**, 179–181
24. Nauli, S. M., Alenghat, F. J., Luo, Y., Williams, E., Vassilev, P., Li, X., Elia, A. E. H., Lu, W., Brown, E. M., Quinn, S. J., et al. (2003) Polycystins 1 and 2 mediate mechanosensation in the primary cilium of kidney cells. *Nat. Genet.* **33**, 129–137
25. Geng, L., Segal, Y., Peissel, B., Deng, N., Pei, Y., Carone, F., Rennke, H. G., Glucksmann-Kuis, A. M., Schneider, M. C., Ericsson, M., et al. (1996) Identification and localization of polycystin, the *PKD1* gene product. *J. Clin. Invest.* **98**, 2674–2682
26. Ikeda, S. R. (1996) Voltage-dependent modulation of N-type calcium channels by G-protein $\beta\gamma$ subunits. *Nature* **380**, 255–258
27. Herlitze, S., Garcia, D. E., Mackie, K., Hille, B., Scheuer, T., and Catterall, W. A. (1996) Modulation of Ca^{2+} channels by G-protein beta gamma subunits. *Nature* **380**, 258–262
28. Lu, W., Shen, X., Pavlova, A., Lakkis, M., Babakhanlou, H., Geng, L., Ward, C., Pritchard, L., Harris, P., Genest, D., et al. (2001) Loss of polycystin-1 leads to defects in epithelial morphogenesis and bone formation. *Hum. Mol. Genet.* **10**, 2385–2396
29. González-Perrett, S., Batelli, M., Kim, K., Essafi, M., Timpanaro, G., Montalbetti, N., Reisin, I. L., Arnaout, M. A., and Cantiello, H. F. (2002) Voltage dependence and pH regulation of human polycystin-2-mediated cation channel activity. *J. Biol. Chem.* **277**, 24959–24966
30. Grimm, D.H., Cai, Y., Chauvet, V., Rajendran, V., Zeltner, R., Geng, L., Avner, E.D., Sweeney, W., Somlo, S. and Caplan, M.J. (2003) Polycystin-1 distribution is modulated by polycystin-2 expression in mammalian cells. *J. Biol. Chem.* **278**, 36786–36793
31. Qian, F., Germino, F. J., Cai, Y., Zhang, X., Somlo, S., and Germino, G. G. (1997) PKD1 interacts with PKD2 through a probable coiled-coil domain. *Nat. Genet.* **16**, 179–183
32. Tsiokas, L., Kim, E., Arnould, T., Sukhatme, V. P., and Walz, G. (1997) Homo- and heterodimeric interactions between the gene products of *PKD1* and *PKD2*. *Proc. Natl. Acad. Sci. USA* **94**, 6965–6970
33. Koulen, P., Cai, Y., Geng, L., Maeda, Y., Nishimura, S., Witzgall, R., Ehrlich, B. E., and Somlo, S. (2002) Polycystin-2 is an intracellular calcium release channel. *Nat. Cell Biol.* **4**, 191–197
34. Luo, Y., Vassilev, P. M., Li, X., Kawanabe, Y., and Zhou, J. (2003) Native polycystin 2 functions as a plasma membrane Ca^{2+} -permeable cation channel in renal epithelia. *Mol. Cell. Biol.* **23**, 2600–2607

35. Vacquier, V. D., and Moy, G. W. (1997) The fucose sulfate polymer of egg jelly binds to sperm REJ and is the inducer of the sea urchin sperm acrosome reaction. *Dev. Biol.* **192**, 125–135
36. Mengerink, K. J., Moy, G. W., and Vacquier, V. D. (2000) The multidomain receptor REJ3 links kidney disease to the sea urchin acrosome reaction. *Mol. Biol. Cell* **11**, 2106
37. Barr, M. M., and Sternberg, P. W. (1999) A polycystic kidney-disease gene homologue required for male mating behaviour in *C. elegans*. *Nature* **401**, 386–389
38. Barr, M. M., DeModena, J., Braun, D., Nguyen, C. Q., Hall, D. H., and Sternberg, P. W. (2001) The *Caenorhabditis elegans* autosomal dominant polycystic kidney disease gene homologs *lov-1* and *pkd-2* act in the same pathway. *Curr. Biol.* **11**, 1341–1346

Received April 25, 2003; accepted December 23, 2003.

Fig. 1

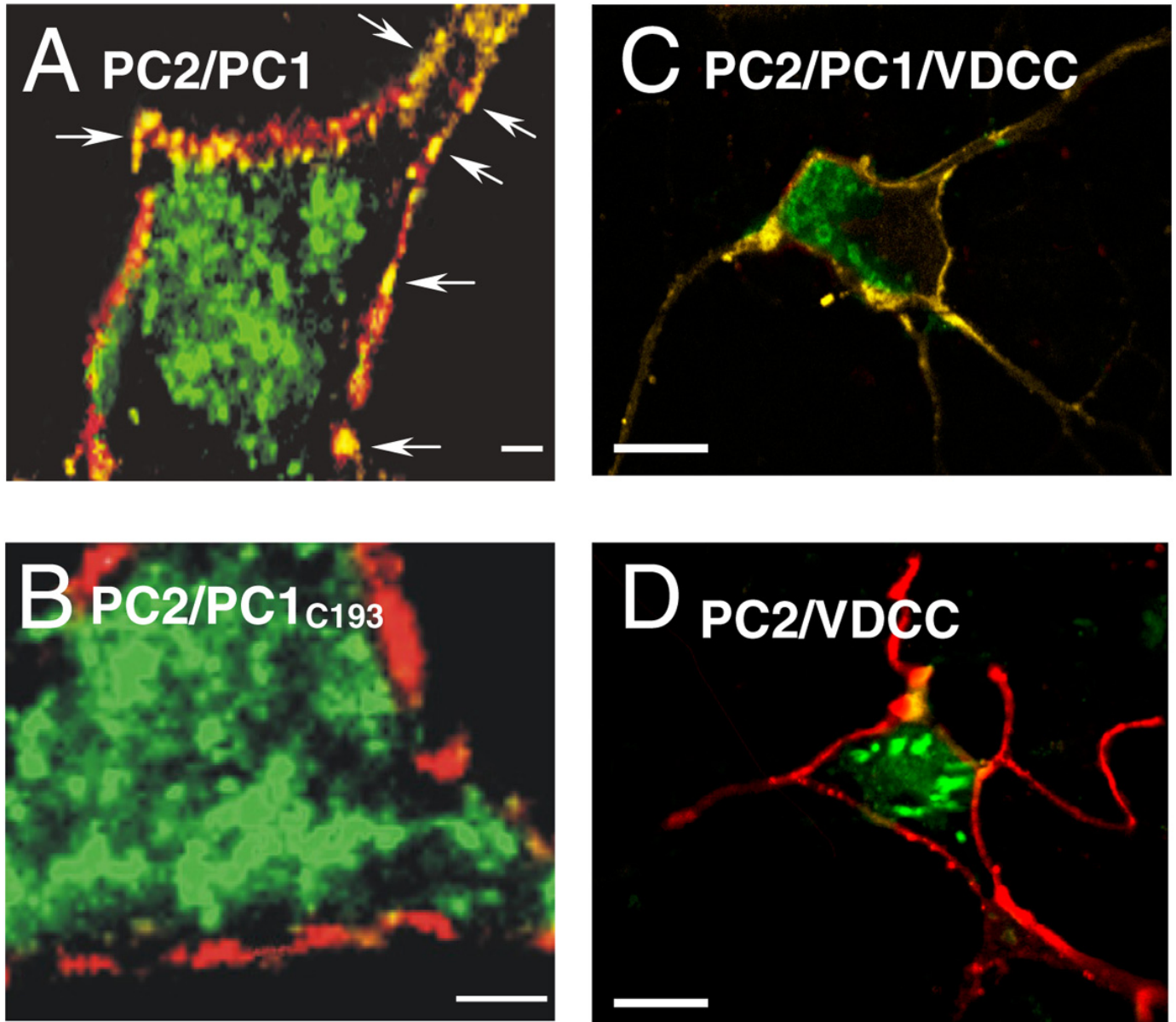


Figure 1. Expression and subcellular localization of polycystin proteins in sympathetic neurons. Confocal images showing combined visualization of mPC2 (green) and PC1 (red) stainings in cells coexpressing mPC2 with either hPC1 (**A**) or the C-terminal mutant mPC1_{C193} (**B**). Note that mPC2 localized at the plasma membrane in the presence of hPC1 (yellow spots and arrows in **A**). Images are 10 μm confocal z axis stacks representative of 24 (**A**) and 19 (**B**) microinjected neurons. Scale bars, 5 μm . **C**, **D**) Confocal images showing combined visualization of sympathetic neurons stained using the anti-mPC2 antibody (green) and an antibody against voltage-dependent N-type Ca^{2+} channels (red). **C**) The neuron was microinjected with mPC2 and hPC1 cDNAs. **D**) The neuron was microinjected with mPC2 alone. Note that mPC2 colocalizes (yellow) at the plasma membrane with the calcium channel only in the cell in which mPC2 and hPC1 are coexpressed. Images are 5 μm confocal z axis stacks representative of 14 (**C**) and 16 (**D**) microinjected neurons. Scale bars, 15 μm .

Fig. 2

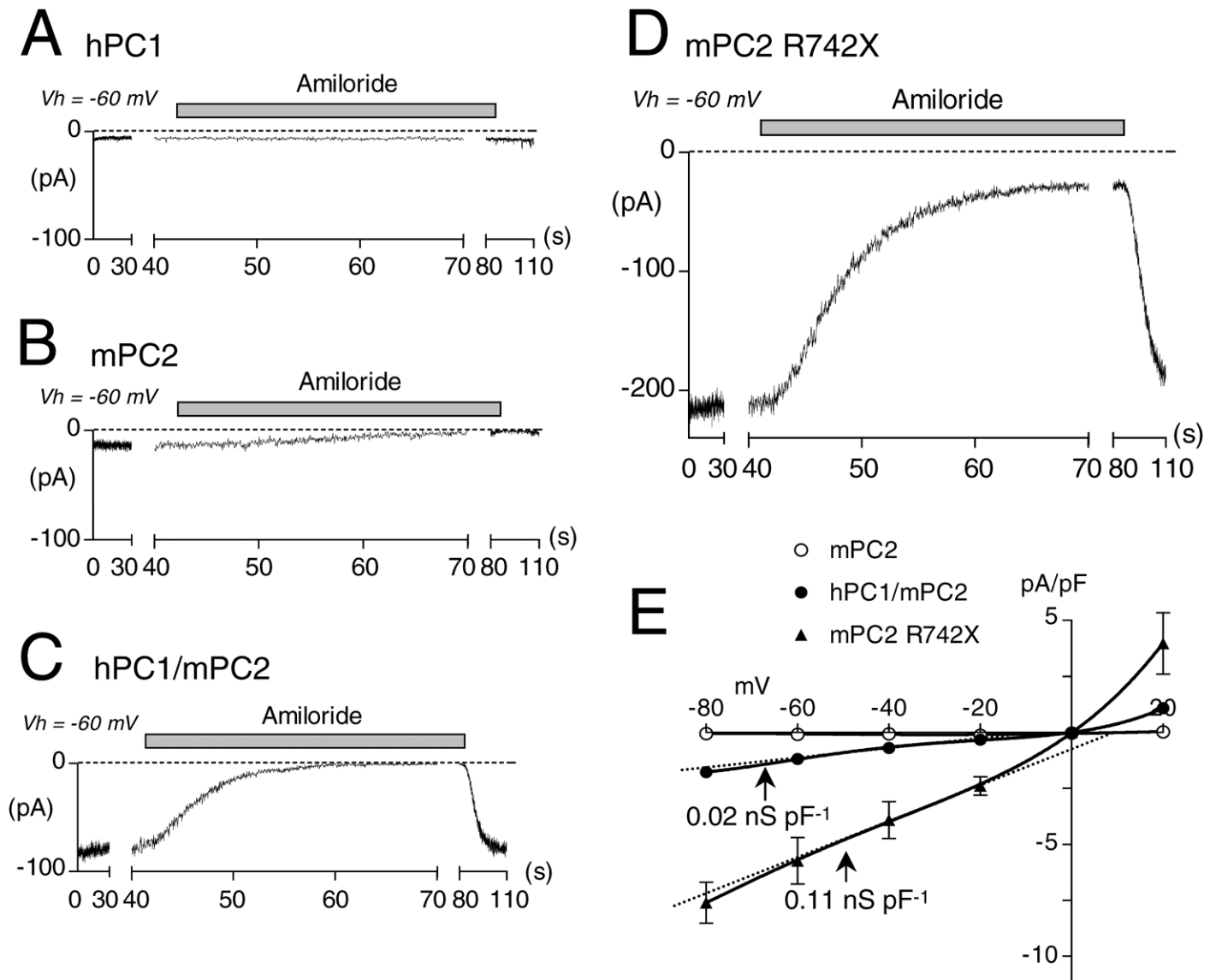


Figure 2. Ion current properties of the PC1/PC2 polycystin complex reconstituted in sympathetic neurons. A–D) Standing inward currents in cells expressing hPC1 (A), mPC2 (B), hPC1/mPC2 (C), and mPC2 R742X (D) as detected from amiloride block (100 μ M). Cells were voltage-clamped at -60 mV using the perforated-patch method. **E)** Current-voltage relationships (normalized to cell capacitance) of the amiloride-sensitive current in cells expressing mPC2 (open circle), hPC1/mPC2 (filled circle), and mPC2 R742X (filled triangle). Points are mean \pm SE ($n=6-8$). The dashed lines are linear regression fits representing the slope conductance extrapolated from the $-60/-40$ mV voltage region. Mean conductance values are given. Note that the mPC2 I-V curve overlaps the x axis.

Fig. 3

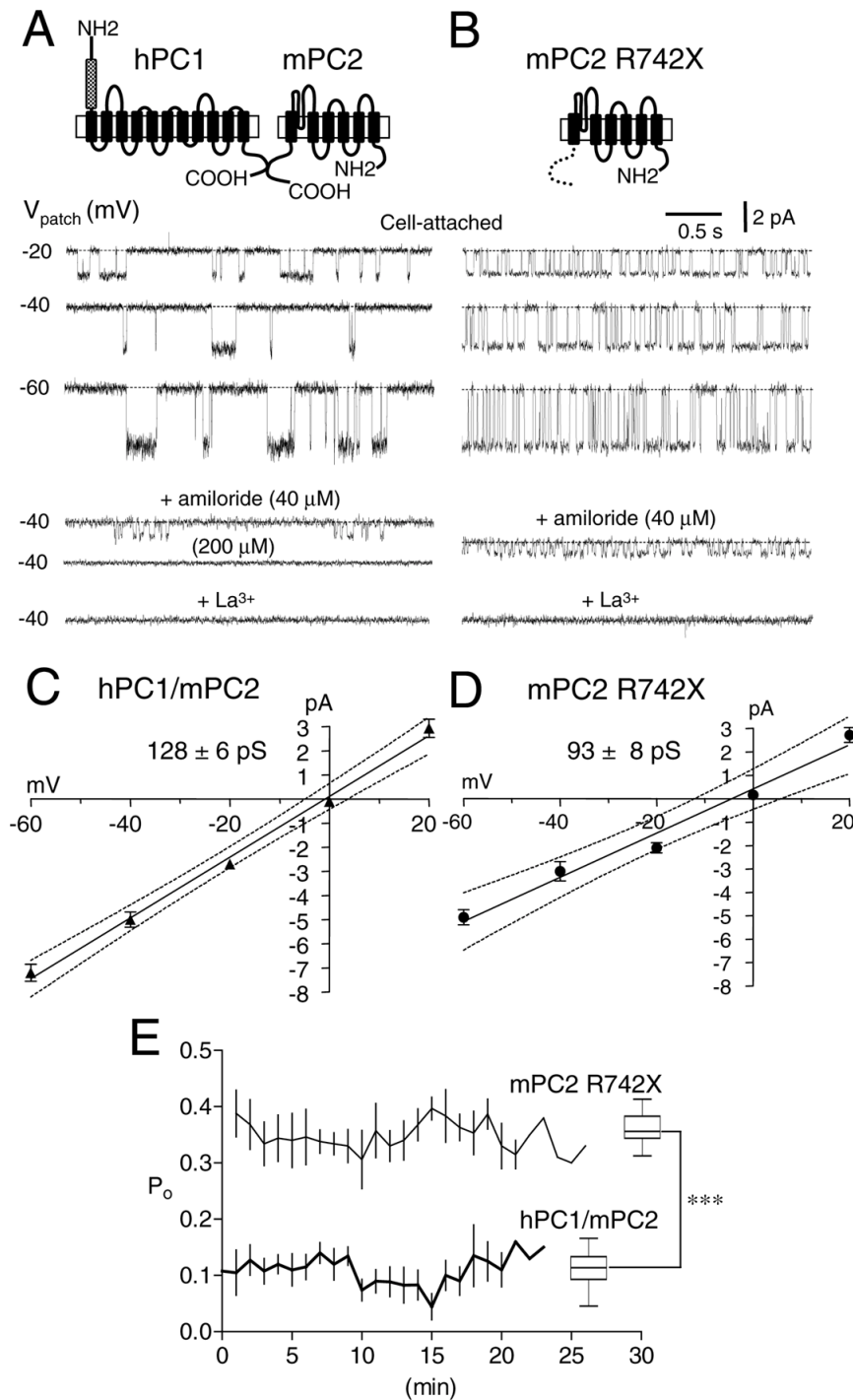


Figure 3. Low open probability of the PC1/PC2 ion channel complex vs. PC2 R742X. Representative single-channel activities recorded from cell-attached patches in cells expressing mPC2/hPC1 (**A**) or mPC2 R742X (**B**) at -20, -40, and -60 mV (V_{patch}). Note the difference in p_o in these two patches. The lower traces show channel activities with amiloride (40 or 200 μM) or La^{3+} (100 μM) added to the patch pipet solution. The pipet solution contained 135 mM Na^+ . Upper panels: schematic illustration of the proposed membrane topology for hPC1, mPC2, and mPC2 R742X. **C**, **D**) Current-voltage relationships for mPC2/hPC1 ($n=8$) (**C**) and mPC2 R742X ($n=6$) (**D**) channel currents. Solid lines are linear regression fits giving slope conductances of 128 ± 6 and 93 ± 8 pS for mPC2/hPC1 and mPC2 R742X, respectively. Dashed lines, 95% confidence limits. **E**) Mean $p_o \pm \text{SE}$ plotted against time for mPC2/hPC1 ($n=6$) and mPC2 R742X ($n=6$) channels. Open probability was calculated per 1-min period in patches containing only one channel. Right panel: box plot summary of the p_o for mPC2/hPC1 and mPC2 R742X cells. *** $P < 0.001$. V_{patch} , -40 mV.

Fig. 4

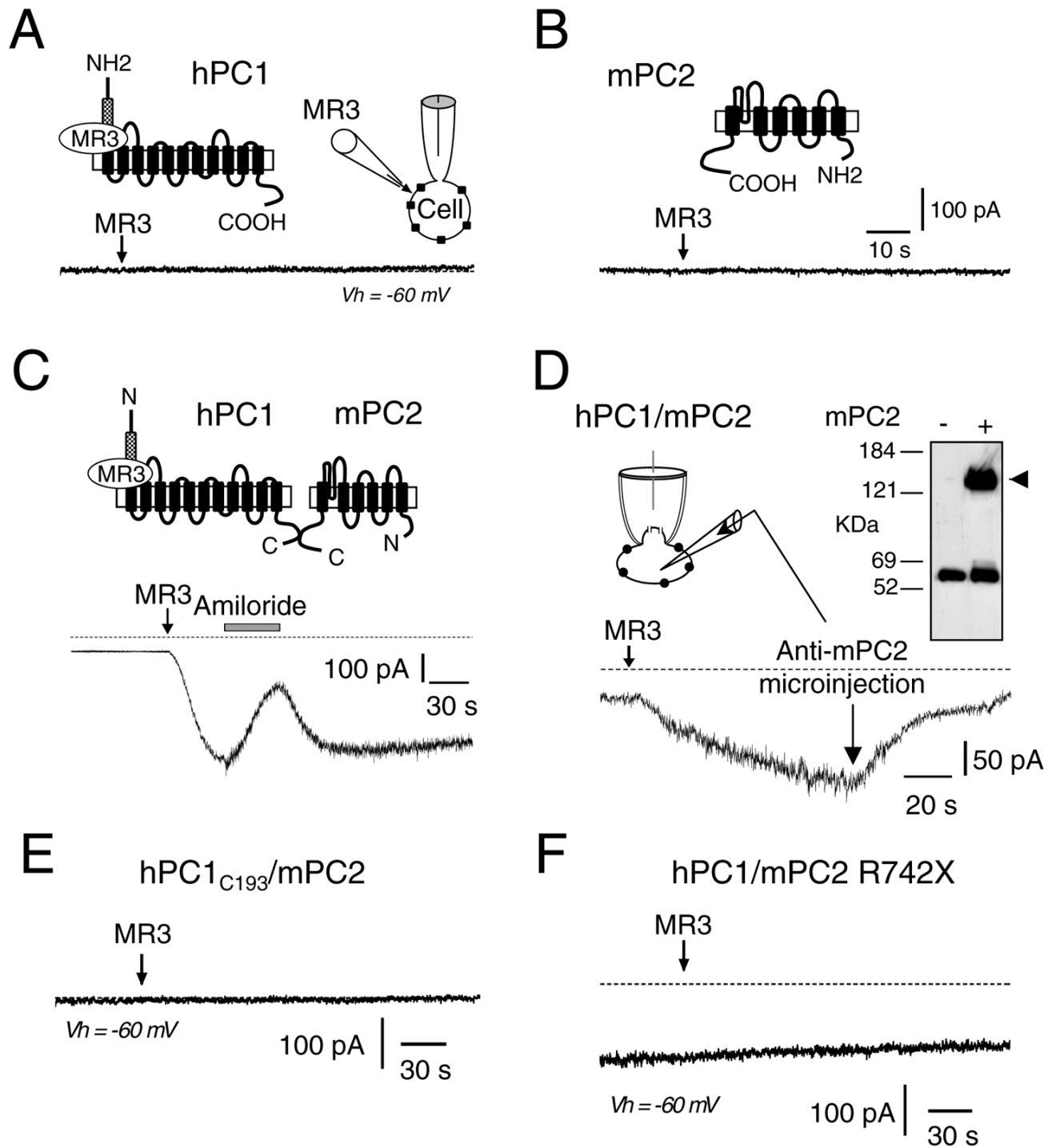


Figure 4. Activation of PC1/PC2 ion channel complex by the MR3 anti-PC1 antibody. Representative inward currents evoked by 10-s application of the MR3 antibody (1/100) in cells expressing hPC1 (**A**), mPC2 (**B**), hPC1/mPC2 (**C**, **D**), hPC1_{C193}/mPC2 (**E**), and hPC1/mPC2 R742X (**F**). Note that MR3 activated an inward current only in hPC1/mPC2-expressing cells (**C**, **D**), which was blocked by bath application of amiloride (80 μ M) (**C**) or cytoplasmic microinjection of the anti-mPC2 antibody (44–62; 1/200) (**D**). Dashes indicate the null-current baseline at –60 mV. (Injection of denatured mPC2 antibody [70°C for 5 min; *n*=6] had no significant effect on MR3 responses.) **D**) Inset: left, schematic diagram of intracellular microinjection of the anti-mPC2 antibody; right, detergent lysates of HEK293 cells transfected (+) or not (–) with myc-tagged mPC2 were immunoprecipitated with anti-myc antibody and blotted with the anti-mPC2 antibody used to block PC2 channel activity. The arrowhead indicates PC2. Note that the lower bands represent reduced heavy chains of the precipitated antibody.

Fig. 5

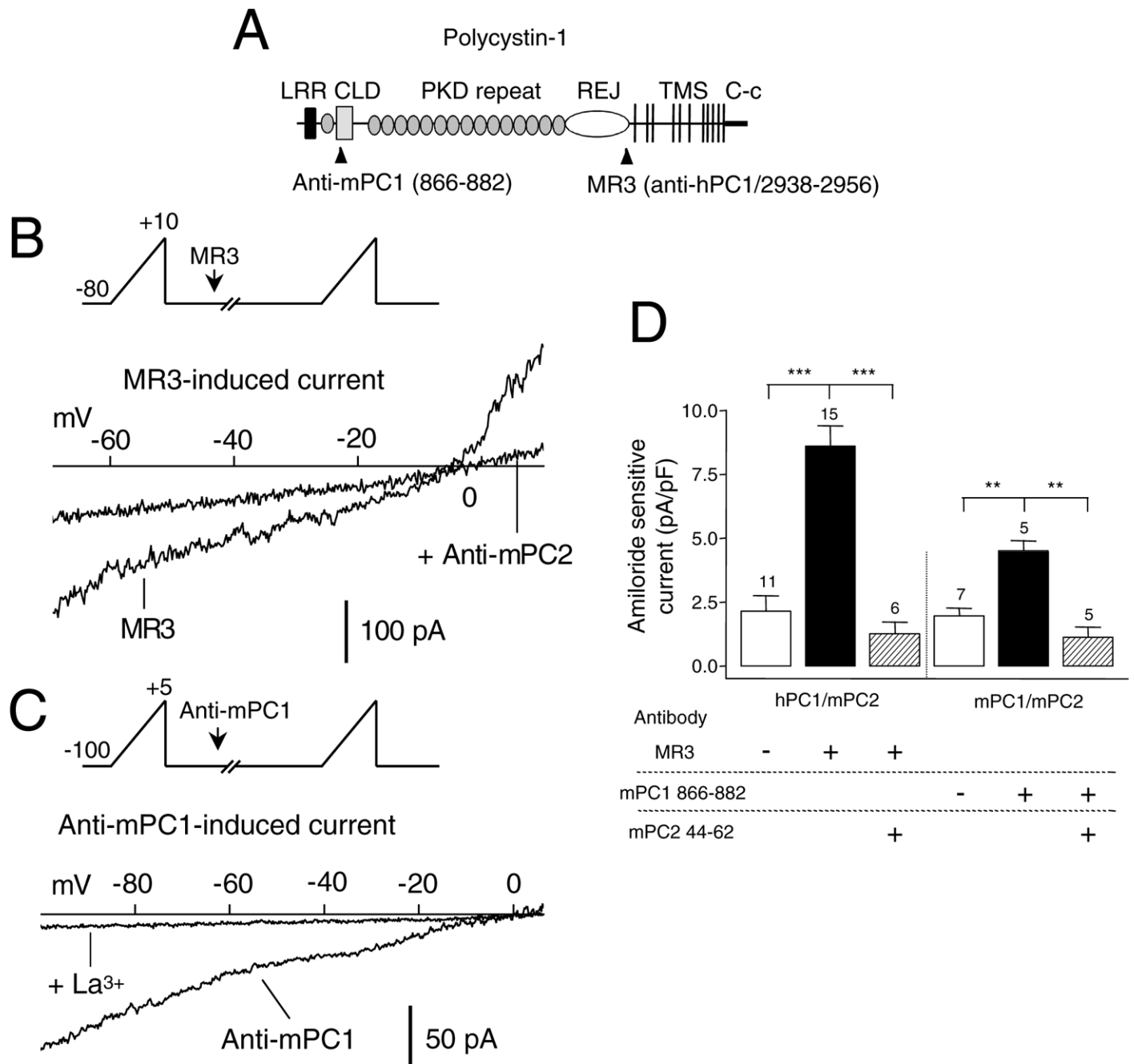


Figure 5. Properties of polycystin ion-channel currents activated by antibodies directed on extracellular domains of PC1. **A**) Schematic representation of the structural organization of PC1 together with the extracellular binding sites of the anti-mPC1 (866-882) and anti-hPC1 (MR3/2938-2956) antibodies used in functional experiments. LRR, leucine rich region; CLD, C-type lectin domain; PKD repeat, polycystin kidney disease repeat; REJ, receptor for egg jelly; TMS, transmembrane segment; C-c, coiled-coil domain. **B, C**) Current-voltage relationships of cation currents evoked by MR3 (**B**) and the mPC1 antibody (**C**). I-V relationships were obtained by subtracting control I-V curves from those in the presence of the antibodies. Voltage-ramps were applied at 20 mV s⁻¹. Note the strong suppression of the inward current by intracellular injection of the anti-mPC2 antibody (1/200) (**B**) and La³⁺ (100 μM) in (**C**). **D**) Summary of the effects of anti-hPC1 and anti-mPC1 antibody applications on cells expressing hPC1/mPC2 or mPC1/mPC2 in the presence (+) or absence (-) of intracellular mPC2 antibody. Bars represent mean ± SE for the number of cells indicated. ***P* < 0.01; ****P* < 0.001.

Fig. 6

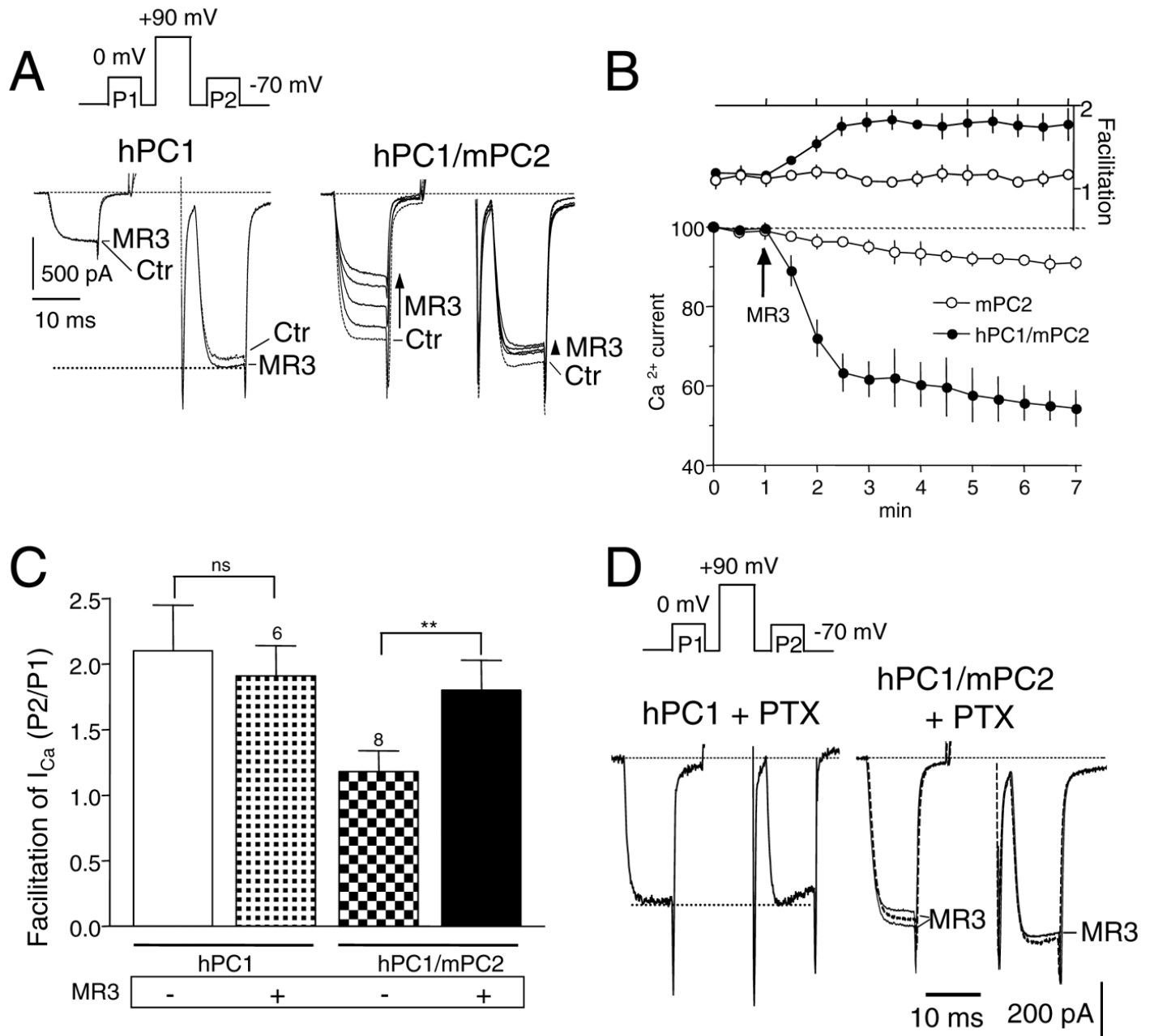


Figure 6. MR3 acting on PC1/PC2 ion channel complexes causes G-protein activation. **A)** Neurons expressing hPC1 (left panel), but not hPC1/mPC2 (right panel), displayed tonic inhibition and voltage-dependent facilitation of N-type Ca²⁺ currents. MR3 had no effect on I_{Ca} in the hPC1-expressing cell but produced voltage-dependent inhibition in the hPC1/mPC2-cell (arrows). Current traces were recorded every 30 s in the right panel. Ca²⁺ currents were evoked at 0 mV before (P1) and after (P2) a depolarizing prepulse to +90 mV as indicated in inset. **B)** Time course of the effects of MR3 on the normalized amplitude (lower panel) and facilitation (upper panel) of the Ca²⁺ current in cells expressing mPC2 (open circle) or hPC1/mPC2 (filled circle). Points are mean ± SE for 5–6 cells. Facilitation was calculated as the ratio of P2 to P1 Ca²⁺ current amplitude. The decay in I_{Ca} amplitude in the mPC2-expressing cell is due to the slow rundown of I_{Ca} typically observed during whole-cell recording. **C)** Summary of facilitation observed in neurons expressing hPC1 or hPC1/mPC2 in the presence (+) or absence (–) of MR3. Bars represent mean ± SE for the number of cells indicated. ns, not significant; **P < 0.01 (paired t tests). **D)** Pertussis toxin treatment prevented the effects of hPC1 on Ca²⁺ currents (left) and blocked the effects of MR3 in a cell expressing hPC1/mPC2 complexes (right) (compare with A). Ca²⁺ currents were evoked as in A.

Fig. 7

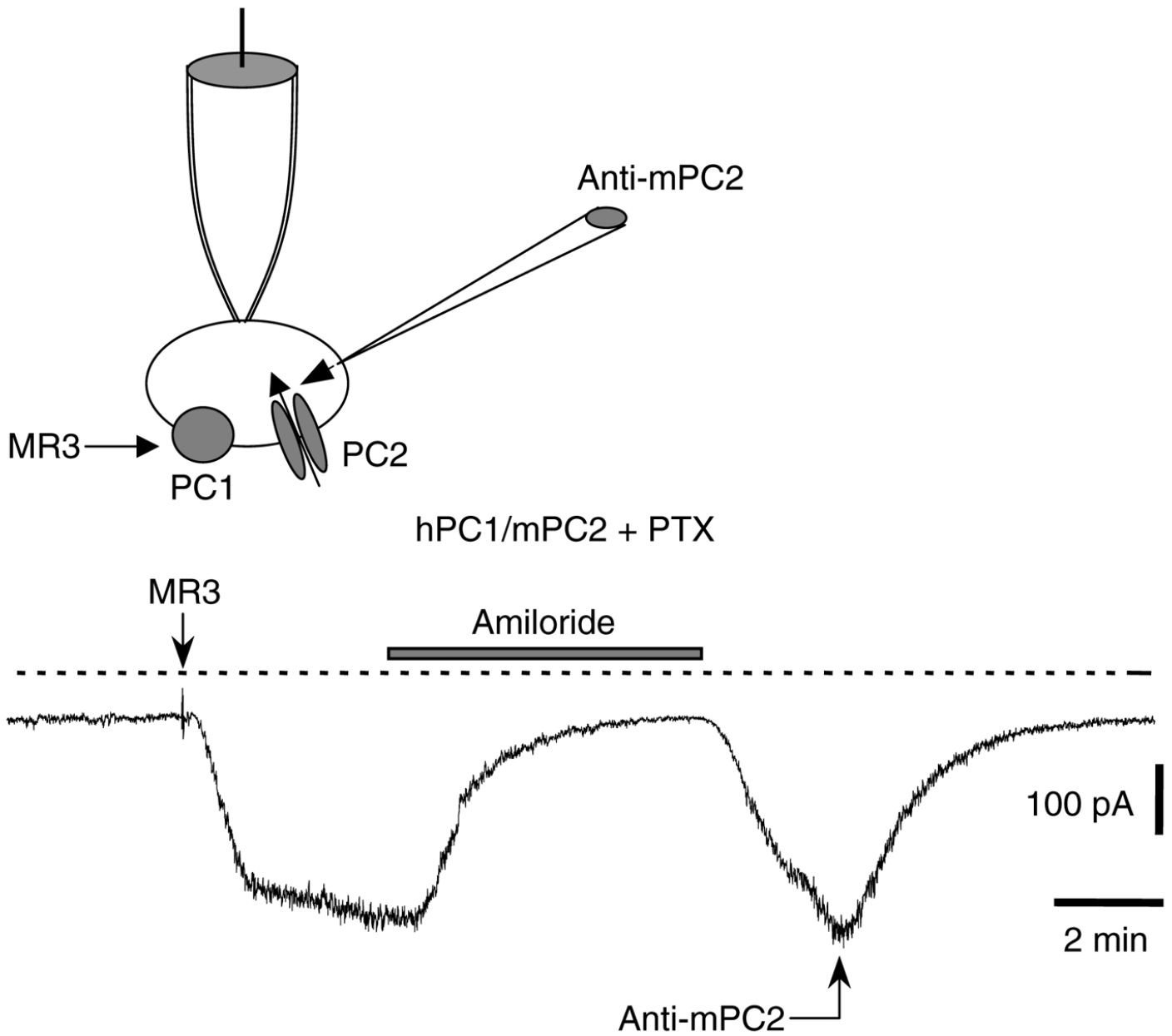


Figure 7. Activation of PC1/PC2 ion-channel complex by MR3 antibody does not depend on G-protein signaling. Activation of hPC1/mPC2 current by MR3 in a cell pretreated with PTX (1 $\mu\text{g}/\text{ml}$ for 24 h). MR3-induced current was blocked by amiloride (100 μM) and by intracellular microinjection of the anti-mPC2 antibody (1/100). Dashes: null-current baseline.

Fig. 8

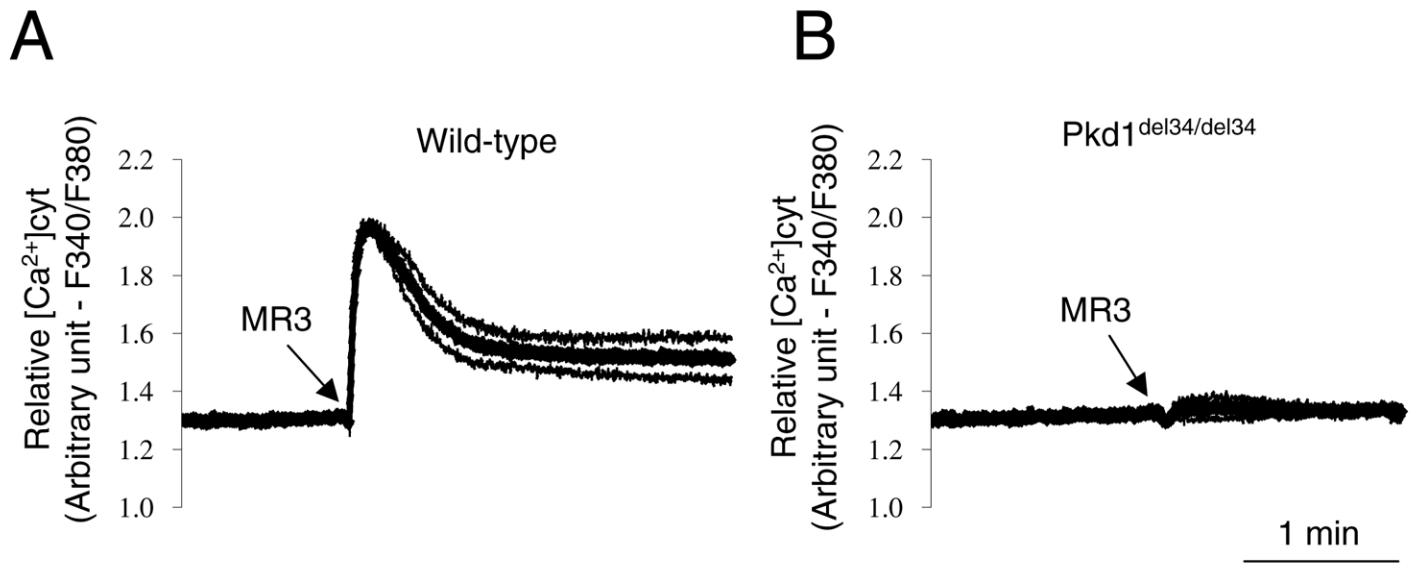


Figure 8. MR3-induced Ca²⁺ mobilization in mouse embryonic kidney cells requires integral PC1/PC2 complexes. Responses to MR3 antibody (1/50 for 10 s) in increases of cytosolic Ca²⁺ are shown for both wild-type (**A**) and *PKD1*^{del34/del34} (**B**) cells. The average (thick lines) and standard errors (thin lines) in response to the application of MR3 antibody are shown. At least two populations of the respective cell lines were used at passages 15 and 16 for each genotype.

Fig. 9

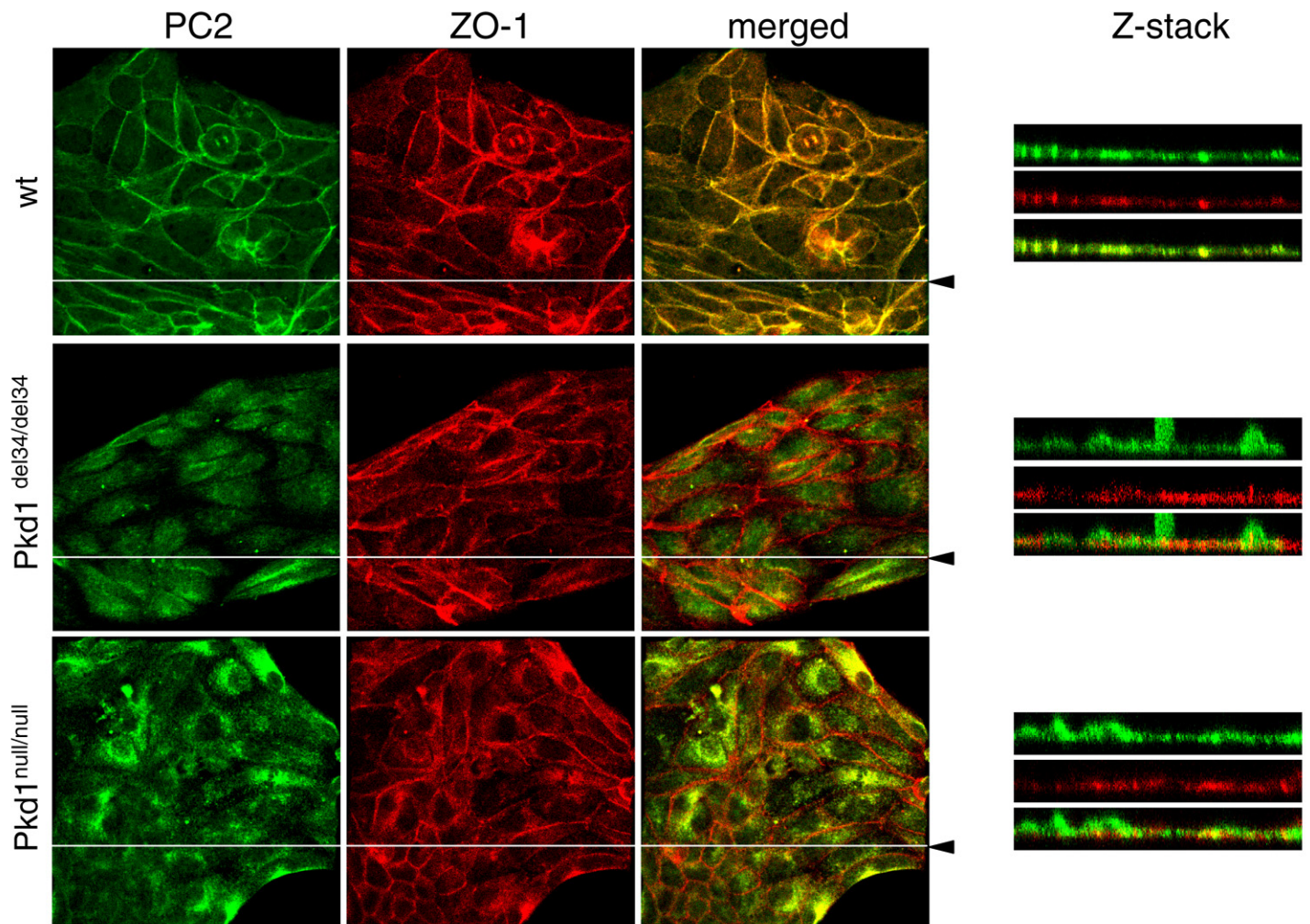


Figure 9. Plasma membrane expression of PC2 requires integral PC1. Confocal images of PC2 and ZO-1 immunostaining in wild-type, *PKD1*^{del34/del34}, and *PKD1*^{null/null} embryonic kidney cells. The merged images and the Z sections demonstrate that membrane localization of PC2 was substantially reduced in *PKD1* mutant kidney cells compared with wild-type cells. Arrow indicates the positions the Z sections were taken.